Cell Research (2017) 27:1293-1297.

www.nature.com/cr

LETTER TO THE EDITOR

Altered neurogenesis and disrupted expression of synaptic proteins in prefrontal cortex of *SHANK3*-deficient non-human primate

Cell Research (2017) **27**:1293-1297. doi:10.1038/cr.2017.95; published online 25 July 2017

Dear Editor,

Despite substantial progress made toward understanding the molecular changes contributing to autism spectrum disorders (ASD), the neuropathophysiology underlying ASD remains poorly understood [1, 2]. Structural brain imaging in humans is valuable, but lacks resolution at the cellular level. Studies of neuropathology in humans have been hampered by the lack of high quality postmortem brains from individuals with ASD [2]. For more than decades, mutant mice have served as major tools to dissect the pathophysiology of ASD because of the wealth of molecular and neurobiological techniques developed for studies with rodents. Our knowledge of molecular and cellular mechanisms for ASD is mostly limited to what we have learned from genetically modified mice. However, there are significant evolutionary differences in brain structure and behavior between rodents and humans. For example, social behaviors and the organization of cerebral cortex differ significantly between primates and rodents. The cerebral neocortex comprises ~80% of the human brain and ~72% of the macaque brain, but only ~28% of the rat brain. Prefrontal cortex (PFC), a critical region for high order cognitive and social functions, is under-developed in rodents compared with primates. The unique behavioral features in human ASD have posed significant challenges to assess the translational value of many findings from ASD mouse models. The apparent evolutionary differences in brain structures and behaviors between mouse and human highlight the need of alternative animal models such as non-human primate models for ASD [3]. The value of a primate model to study ASD has been supported by the generation and characterization of monkeys with altered expressions of *MECP2* using the lentivirus- and TALEN-based method [4, 5].

Mutations in human *SHANK3* remain one of the best-replicated and well-characterized genetic defects in ASD. Various types of mutations in *SHANK3* have been found in ~1% of individuals with ASD [6]. SHANK3 protein is one of the three-member family proteins (SHANK1-3) known to function as postsynaptic scaffolding proteins in excitatory synapses. So far, a total of 14 independent lines of *Shank3*-mutant mice have been reported, but none of these studies focused on the neuropathology in the prenatal brain [6, 7]. These mutant mice display a spectrum of behavioral phenotypes. However, interpretation of the behavioral phenotypes in rodent models relevant to the *SHANK3*-related disorders remains a challenge. For these reasons, *SHANK3* represented a unique opportunity to test the feasibility of generating an ASD model in non-human primates.

We used the Cas9/sgRNA method to disrupt *SHANK3* gene in cynomolgus monkeys (*Macaca fascicularis*) following previous protocols [8, 9]. *SHANK3* has an array of mRNA isoforms due to multiple promoters and extensive alternative splicing of coding exons in both human and rodent, and this pattern is expected to be conserved in non-human primates [5, 10]. We therefore simultaneously targeted two sites (exons 6 and 12) of *SHANK3* to induce a large deletion (Figure 1A and Supplementary information, Figure S1A) that could completely disrupt all SHANK3 isoforms. We selected sgRNAs that showed high targeting efficiency for injection into monkey embryos.

We obtained 3 pregnancies after transferring 116 injected embryos to 37 surrogate mothers (Figure 1B). The pregnancy rate of 8.1% (3/37) was significantly lower than that of other targeted genes (34.5%) performed in the same center under the same experimental conditions (Li X *et al*., unpublished data). The reason for the low pregnancy rate is currently unknown, but suggests that SHANK3 expression might be important for early development in primates. Of three monkey offsprings, one miscarried close to the term gestation (125 days) ($SHANK3^{M1}$), one was lost due to a difficult labor ($SHANK3^{M2}$), and one is still alive ($SHANK3^{M3}$) (Supplementary information, Figure S1B). There are

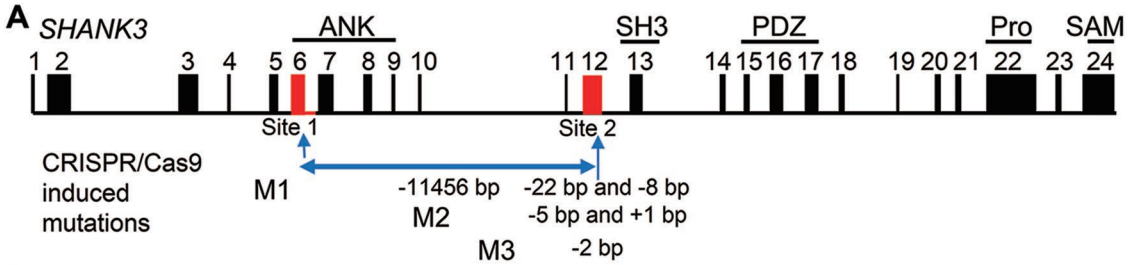

B

No. embryos transferred	Pregnancy /Surrogates	Stillbirth /miscarriage	Live birth	Mutation (%)
116	3/37 (8.1%)	1/1	1	3 (100%)

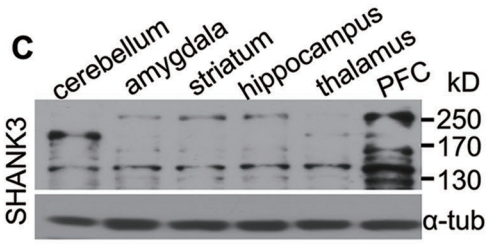

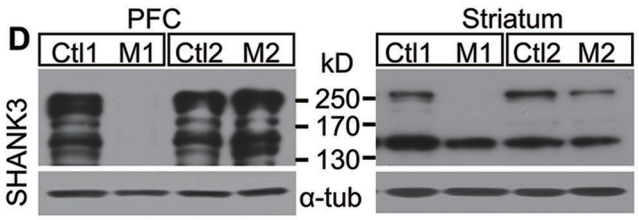

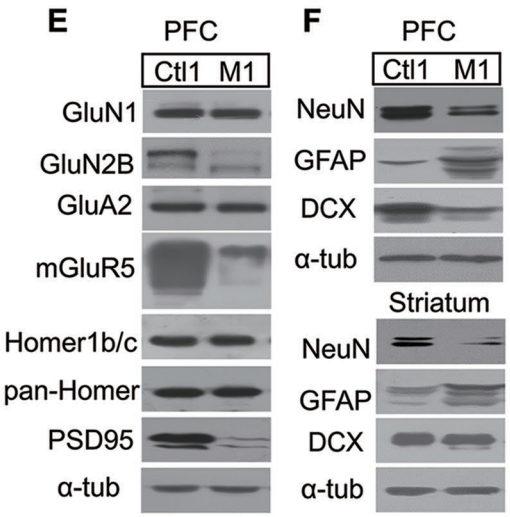

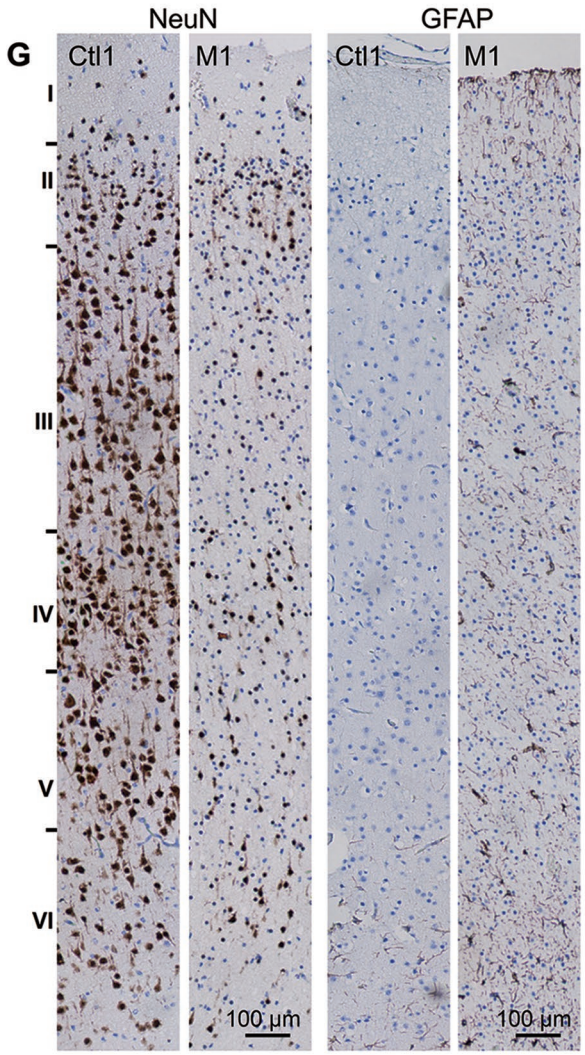

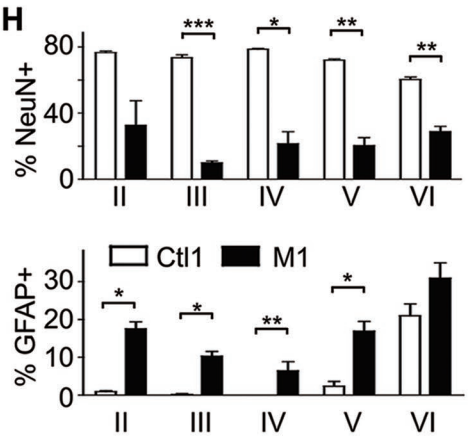

Figure 1 Generation and phenotypic analysis of *SHANK3*-mutant cynomolgus monkeys. **(A)** Schematic diagram of *Macaca fascicularis SHANK3* gene, protein domains, Cas9/sgRNA targeting sites in exons 6 and 12, and confirmed mutations of *SHANK3* in *SHANK3*$^{M1\text{-}M3}$ animals. The gene structure of monkey *SHANK3* was deduced from the mRNA of XM_015456961 and a genomic contig of NC_022281 for *SHANK3*. **(B)** Summary of embryo transplantation and surrogacy in cynomolgus monkeys. **(C)** Brain region-specific expression profile of SHANK3 protein in wild-type P0 monkey. SHANK3 displays isoform-specific expression in different brain regions and is expressed at the highest level in PFC. **(D)** Western blot analysis of SHANK3 protein in the PFC and striatum of *SHANK3*-mutant monkeys. Ctl1 and Ctl2 are age-matched controls at gestational day 135 and full-term gestation, respectively. **(E)** Altered expressions of postsynaptic receptors and scaffold proteins in *SHANK3*^{M1} brain. Normal expressions of GluN1, GluA2, Homer1b/c, and pan-Homer but decreased expressions of GluN2B, mGluR5, and PSD95 were observed in the PFC of *SHANK3*^{M1}. **(F)** Western blot analysis of NeuN, GFAP, and DCX in whole-cell lysates from PFC. *SHANK3*^{M1} showed decreased levels of NeuN and DCX but increased level of GFAP in the PFC. Western blot analysis was repeated at least three times independently. **(G)** NeuN and GFAP staining (brown) in layers I-VI of PFC. NeuN staining showed a strong signal in the nucleus and a weak signal in the cytosol. Nuclei were stained with hematoxylin (blue). There were fewer NeuN+ neurons and more GFAP+ astrocytes in the PFC of *SHANK3*^{M1}. Scale bar, 100 μm. **(H)** Percentages of NeuN+ neurons and GFAP+ astrocytes in each layers of PFC. $n = 6$, $^{*}P < 0.05$, $^{**}P < 0.01$, and $^{***}P < 0.001$ by Student's *t*-test.

no apparent developmental defects in *SHANK3*^{M1} and *SHANK3*^{M2} fetuses to explain their death. The brain and other somatic tissues of *SHANK3*^{M1} and *SHANK3*^{M2}, and selected somatic tissues of *SHANK3*^{M3} were analyzed for targeted mutations at sites 1 and 2. All three offsprings were positive for mutations at site 2 of exon 12 (−22 and −8 bp in *SHANK3*^{M1}, −5 and +1 bp in *SHANK3*^{M2}, and −2 bp in *SHANK3*^{M3}; Supplementary information, Figure S1C-S1F). A large deletion was detected in different tissues of *SHANK3*^{M1} with a pair of primers spanning sites 1 and 2, as evidenced by a positive band around 500 bp (Supplementary information, Figure S1C). Sequencing of this band confirmed an 11 456 bp deletion between the two targeting sites (Supplementary information, Figure S1E). The small indels in different mutant animals were confirmed by deep amplicon sequencing (Supplementary information, Figure S1F). However, deep amplicon sequencing was unable to detect the large 11 456 bp deletion. Using the semi-quantitative PCR analysis of genomic DNA, we estimated that ~70% of the alleles carry the large deletion in *SHANK3*^{M1}, which is predicted to disrupt the expression of most SHANK3 isoforms based on the transcript pattern of *SHANK3* in human and rodent [6, 10]. Off-target analysis did not reveal any additional mutations (Supplementary information, Figure S1G).

The brain tissues from *SHANK3*^{M1} and *SHANK3*^{M2} provided a unique opportunity to investigate *SHANK3* mutation-associated neuropathology. *Shank3* displays a temporal- and spatial-specific expression for its isoforms in mouse brain with peak expression in striatum of postnatal day 14 (P14) brain (Supplementary information, Figure S2). In contrast, we found that SHANK3 showed the highest level of expression in the PFC of monkey at birth (P0), a developmental time point that corresponds to P14 in mice (Figure 1C). The distinct expression patterns of SHANK3 in mouse and monkey brains may reflect the evolutionary differences between the two species.

We performed western blot analysis using whole-cell lysates isolated from different brain regions of mutants and age-matched controls (Ctl1 for *SHANK3*^{M1} and Ctl2 for *SHANK3*^{M2}) using an antibody against the C-terminus of mouse Shank3 that is predicted to detect most, if not all, SHANK3 isoforms of primates (Figure 1D) [11]. Compared to the control, no SHANK3 protein isoforms were detected in the cortex of *SHANK3*^{M1} animal, indicating a complete loss of SHANK3 resulting from the 11 kb, 22 and 8 bp deletions in the PFC (Figure 1D). In contrast, an isoform-specific deficiency of SHANK3 was revealed in the striatum of *SHANK3*^{M1} animal, in which the full-length isoform was absent but a short isoform was still present. In the *SHANK3*^{M2} brain, the full-length SHANK3 was decreased to a greater extent than the short isoform in the striatum. Interestingly, the majority of isoforms were not decreased but mildly increased in the cortex presumably by a compensatory mechanism. These findings are generally consistent with the mosaic nature of CRISPR/Cas9-mediated gene editing, which accounts for the various extents of disruption of the targeted gene in different brain regions. However, the isoform-specific expression of SHANK3 in different brain regions should also be considered.

Given the alteration of SHANK3-interacting proteins in *Shank3*-deficient mice [6, 7], we selected several synaptic proteins for western blot analysis in *SHANK3*-deficient monkey brain (Figure 1E, Supplementary information, Figure S3A and S3B). We found no apparent difference in the levels of GluN1, GluA2, Homer1b/c, and pan-Homer in the PFC between *SHANK3*^{M1} and control. However, a significant decrease was revealed for mGluR5 (54.7% ± 10.6% of ctl1, $n = 5$, mean ± SEM), GluN2B (18% ± 6.8%, $n = 3$), and PSD95 (15.5% ± 2.6%, $n = 6$) in the PFC of *SHANK3*^{M1} compared to the control. In striatal neurons of *Shank3*-deficient mice, Homer1b/c abnormally accumulates in the cytoplasm despite no significant increase in overall proteins [11]. Consistently, more

cytoplasmic staining of Homer1b/c was also observed in PFC neurons of *SHANK3*^{M1} animal compared with its control (Supplementary information, Figure S4A and S4B). We further co-stained SHANK3 and PSD95, and found apparent reductions in the staining intensity of the two proteins in the PFC of *SHANK3*^{M1} (Supplementary information, Figure S5A), consistent with the western blot results (Figure 1D and 1E). The loss of SHANK3 and alterations in its interacting proteins in *SHANK3*^{M1} brain verify the findings from other species [11, 12].

The abundant expression of SHANK3 in the control but a complete loss of SHANK3 in the PFC of the *SHANK3*^{M1} animal led us to focus on the pathological outcome in this brain region. Immunohistochemical analysis revealed that the structure of cortical layers is comparable between *SHANK3*^{M1} and its control. While the cell density of cortical layers did not differ between control and mutant PFCs, the cell bodies of *SHANK3*^{M1} were smaller (Figure 1G). Strikingly, we found significantly fewer NeuN+ neurons in the PFC of *SHANK3*^{M1} (72.2% ± 1.2% NeuN+ cells/total cell counts for Ctl1 and 22.7% ± 5% for *SHANK3*^{M1}; Figure 1G and 1H) with reduced soma size (48.0 ± 10.2 μm^2 NeuN+ cell for Ctl1 and 22.7 ± 4.8 μm^2 for *SHANK3*^{M1}, n = 6 slices). On the contrary, there were significantly more GFAP+ astrocytes in the PFC of *SHANK3*^{M1} animal compared to the control (Figure 1G and 1H) based on quantitative analysis of DAB staining results. Double immunofluorescent staining confirmed fewer NeuN+ cells in the PFC and the increased GFAP-labeling in the PFC and striatum of *SHANK3*^{M1} brain (Supplementary information, Figure S4C and S4D). The histological studies of *SHANK3*^{M2} did not reveal any apparent abnormalities in the PFC (Supplementary information, Figure S5B), consistent with the finding of no apparent loss of SHANK3 in *SHANK3*^{M2} brain. The fewer NeuN+ neurons and more GFAP+ astrocytes in the PFC of *SHANK3*^{M1} were further supported by western blot analysis (Figure 1F). Specifically, the NeuN protein was markedly reduced (25% ± 8.7%, n = 5), whereas the GFAP protein was significantly increased (357% ± 144%, n = 5) in *SHANK3*^{M1} PFC compared to control (Supplementary information, Figure S3C). Western blot analysis also showed a decreased level of Doublecortin (DCX; 65% ± 3.7%, n = 3), a marker of progenitor neurons, in the PFC, but a normal level in the striatum of *SHANK3*^{M1} brain (Figure 1F and Supplementary information, Figure S3C). These results together suggest a brain region-specific neurogenesis defect in *SHANK3*^{M1} mutants.

Given the altered synaptic receptors and PSD proteins in *SHANK3*^{M1} brain, we used Golgi impregnation method to examine dendritic spines in the PFC of *SHANK3*^{M1} and *SHANK3*^{M2} brains and observed a significant decrease in dendritic spine density of the *SHANK3*^{M1} but not *SHANK3*^{M2} mutants compared to control, whereas the length from the tip to the base of a spine was not significantly altered in both mutant animals (Supplementary information, Figure S6). These results are consistent with previous reports in *Shank3*-mutant mice or neurons derived from *SHANK3*-deficient patients documenting a reduced spine density [11, 12].

In summary, we successfully introduced various types of deleterious mutations in *SHANK3* for the first time in cynomolgus monkeys by the CRISPR/Cas9 genome editing method. *SHANK3*-deficient fetus showed a significant loss of NeuN+ neuronal cells accompanied with an increase of GFAP+ astrocytes, which has not been found in any line of *Shank3*-knockout mice, demonstrating a unique and critical role of SHANK3 in early brain development in primates. SHANK3 has been known as a scaffolding protein in synapses. However, our findings suggested an important role of SHANK3 in early developing brains in non-human primate. The mechanism by which SHANK3 regulates neurogenesis, in addition to the conventional synaptic function, in the prenatal brain remains to be elucidated. Our findings from *SHANK3*-deficient monkey predict that similar but milder changes may underlie the pathophysiology of human individuals with *SHANK3* haploinsufficiency. The defects in early brain development and the reduced size of neuron soma are reminiscent of the neuronal defects in MeCP2 and PTEN ASD mouse models [1]. The pattern of molecular changes resulting from the *SHANK3* deficiency is overall conserved between mouse and monkey brains, but the pathological changes are more prominent in *SHANK3*-deficient monkey. While these findings support the value of mouse models, they also underscore the importance of using non-human primates to model *SHANK3* and other gene mutations causing ASD.

Materials and Methods are available in Supplementary information, Data S1, Tables S1 and S2.

Acknowledgments

We thank Drs Weixiang Guo, Xiaoming Wang and Zhiheng Xu for discussion, Ruxiao Xing, Xudong Liu and Jinquan Gao for technical assistance, Yafeng Luo (Guangzhou Yuanxi Biotech Co., Ltd) for animal resource and care, and Samuel Hulbert for critical reading of the manuscript. The project was supported by the Ministry of Science and Technology of China (2014CB942803 and 2016YFA0501000), the Strategic Priority Research Program of the Chinese Academy of Sciences (XDB02020400), and the National Natural Science Foundation of China (31110103907, 91332206 and 31490592).

Hui Zhao[1, 2, *], Zhuchi Tu[1, 3, *], Huijuan Xu[1], Sen Yan[3], Huanhuan Yan[4], Yinghui Zheng[1], Weili Yang[3],

Jiezhao Zheng[5], Zhujun Li[5], Rui Tian[1], Youming Lu[4], Xiangyu Guo[3], Yong-hui Jiang[6], Xiao-Jiang Li[1, 3, 7], Yong Q Zhang[1, 2]

[1]State Key Laboratory of Molecular Developmental Biology, Institute of Genetics and Developmental Biology, Chinese Academy of Sciences, Beijing 100101, China; [2]University of Chinese Academy of Sciences, Beijing 100101, China; [3]Guangdong-Hongkong-Macau Institute of CNS Regeneration, Ministry of Education CNS Regeneration Collaborative Joint Laboratory, Jinan University, Guangzhou, Guangdong 510632, China; [4]The Institute for Brain Research, Collaborative Innovation Center for Brain Science, Huazhong University of Science and Technology, Wuhan, Hubei 430030, China; [5]Yuanxi Biotech Inc., Guangzhou, Guangdong 5010663, China; [6]Department of Pediatrics and Department of Neurobiology, Duke University, Durham, NC 27710, USA; [7]Department of Human Genetics, Emory University School of Medicine, Atlanta, GA 30322, USA

*These two authors contributed equally to this work.

Correspondence: Yong-hui Jiang[a], Xiao-Jiang Li[b], Yong Q Zhang[c]

[a]E-mail: yong-hui.jiang@duke.edu

[b]E-mail: xli2@emory.edu

[c]E-mail: yqzhang@genetics.ac.cn

References

1 de la Torre-Ubieta L, Won H, Stein JL, *et al. Nat Med* 2016; **22**:345-361.
2 Amaral DG, Schumann CM, Nordahl CW. *Trends Neurosci* 2008; **31**:137-145.
3 Watson KK, Platt ML. *J Neurodev Disord* 2012; **4**:21.
4 Chen Y, Yu J, Niu Y, *et al. Cell* 2017; **169**:945-955.
5 Liu Z, Li X, Zhang JT, *et al. Nature* 2016; **530**:98-102.
6 Jiang YH, Ehlers MD. *Neuron* 2013; **78**:8-27.
7 Monteiro P, Feng G. *Nat Rev Neurosci* 2017; **18**:147-157.
8 Tu Z, Yang W, Yan S, *et al. Sci Rep* 2017; **7**:42081.
9 Niu Y, Shen B, Cui Y, *et al. Cell* 2014; **156**:836-843.
10 Zhu L, Wang X, Li XL, *et al. Hum Mol Genet* 2014; **23**:1563-1578.
11 Wang X, Bey AL, Katz BM, *et al. Nat Commun* 2016; **7**:11459.
12 Shcheglovitov A, Shcheglovitova O, Yazawa M, *et al. Nature* 2013; **503**:267-271.

(**Supplementary information** is linked to the online version of the paper on the *Cell Research* website.)